*Papers submitted to the Conference "Applications of Physics in Mechanical and Material Engineering"*

# Numerical Modeling of Precipitation Processes in Heat Resistant HR3C Austenitic Steel Using CALPHAD Method

H. Purzyńska[a,*], R. Kuziak[a] and G. Golański[b]

[a] *Łukasiewicz Research Network — Institute for Ferrous Metallurgy, K. Miarki 12-14, 44-100 Gliwice, Poland*
[b] *Czestochowa University of Technology, al. Armii Krajowej 19, 42-200 Częstochowa, Poland*

Doi: 10.12693/APhysPolA.142.145 *e-mail: hanna.purzynska@imz.pl

The paper deals with numerical modelling of precipitation processes in HR3C austenitic steel used in supercritical power units. Thermodynamic and kinetic modelling was performed using, respectively, ThermoCalc and TC-PRISMA software. Both programmes use the CALculation of PHAse Diagrams method. The thermodynamics calculations predicted the formation of $M_{23}C_6$ carbide, $\sigma$-phase and Z-phase in HR3C steel at working temperatures of power units. Verification of the modelling stage was performed by ageing the steel samples at 700°C for 100 and 500 h. It was found that during a such short time of ageing, $M_{23}C_6$ carbide precipitated mainly at austenite grain boundaries, while NbX and Z-phase particles precipitated inside the grain.

topics: modelling, ThermoCalc, TC-Prisma, austenitic steel

## 1. Introduction

The HR3C steel is well known and widely used creep resistant austenitic steel. High resistance to creep, as well as high-temperature corrosion and oxidation resistance in steam, makes this steel a suitable material for the components of supercritical power units, including, for example, boiler superheaters working at 650–660°C [1]. The excellent properties of HR3C steel are related to its chemical composition giving rise to the solid solution and precipitation strengthening. The performance of this steel may be further improved by modifying the chemical composition targeting at the atoms' interaction in the solid solution and modifying the kinetics of precipitations processes occurring during the heat treatment and under the service conditions.

Recent advances in computational thermodynamics allow for an accurate description of the behaviour of complex systems. Accordingly, the thermodynamic and kinetic modelling of phase diagrams is widely used to design the chemical composition as well as the heat treatment conditions of new materials. In general, the approaches used for this purpose include atomistic and continuum models. Atomistic models are computational tools for modelling the collective behaviour of atoms in larger systems, including molecules and crystals [2]. In the continuum methods of modelling, the complex systems are represented by phenomenological continuous functions [3]. The viability of using the continuous function to describe complex systems was first recognised at the beginning of the twentieth century [4, 5]. However, a substantial progress in computational techniques is dated from the works of Kaufman [6]. The aim of this paper is to present the capability of the CALPHAD (CALculation of PHAse Diagrams) method to predict the behaviour of HR3C steel during ageing at 700°C.

## 2. Research methodology

The test material was HR3C austenitic stainless steel with the chemical composition presented in Table I. The test specimens were taken from a pipe section with dimensions of $50.1 \times 12.5$ mm$^2$ and then subjected to ageing at 700°C for up to 500 h.

Thermodynamic and kinetic modelling was performed using, respectively, ThermoCalc and TC-PRISMA software. Both programmes use the CALPHAD method. The calculations presented in this paper were performed using the ThermoCalc software (v. 2022a) and the database TCFE11.

TABLE I
Chemical composition of HR3C steel [%].

| C | Si | Mn | P | S | Cr | Nb | Ni | N |
|---|---|---|---|---|---|---|---|---|
| 0.10 | 0.40 | 0.74 | 0.018 | 0.001 | 24.80 | 0.30 | 22.10 | 0.25 |

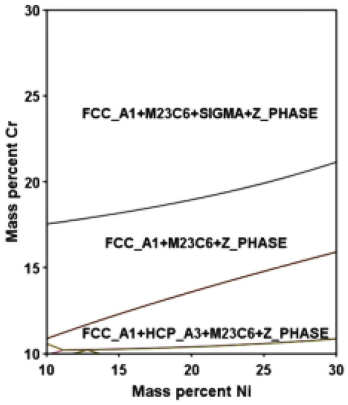


Fig. 1. Isoplethal section of the phase diagram for HR3C steel at 700°C.

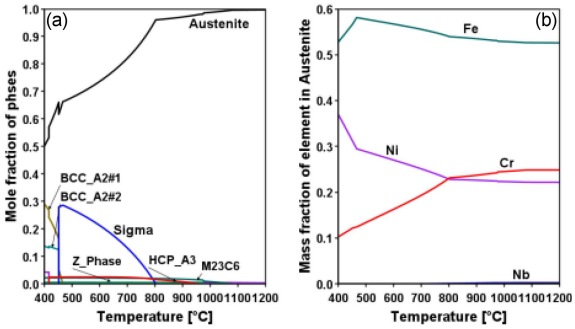


Fig. 2. Variation of (a) equilibrium mole fractions of phase constituents and (b) chemical composition of austenite in HR3C steel as a function of temperature.

The microstructure investigation was carried out using the Jeol JSM 6610LV scanning electron microscope (SEM). The precipitations were identified using the FEI Titan 80-300 transmission electron microscope (TEM).

## 3. Results

### 3.1. Thermodynamic simulations using ThermoCalc

In the beginning, the effect of crucial components, Cr and Ni, on the phase boundaries was calculated at 700°C (Fig. 1).

In the calculations, all elements of HR3C steel, with the exception of Cr and Ni, were fixed. The calculated set of the stable phases for the chemical composition of the steel include FCC_A1 (Austenite), $M_{23}C_6$, $\sigma$-phase, Z-phase, and HCP_A3 phase. The dependence of the mole fraction of phase constituents in the equilibrium of HR3C steel on temperature is shown in Fig. 2. The most important phases for the performance of this steel include $M_{23}C_6$ carbide, $\sigma$-phase, and Z-phase. The process of their formation is accompanied by the depletion of the austenite matrix in chromium (Fig. 2b).

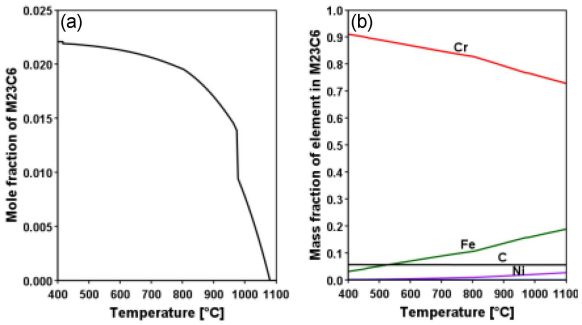


Fig. 3. Variation of (a) equilibrium mole fraction and (b) chemical composition of $M_{23}C_6$ in HR3C steel, as a function of temperature.

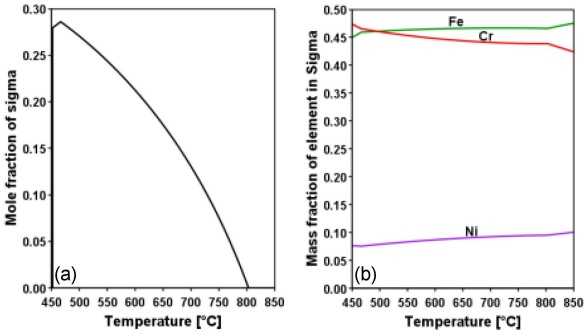


Fig. 4. Variation of (a) equilibrium mole fraction and (b) chemical composition of $\sigma$-phase in HR3C steel, as a function of temperature.

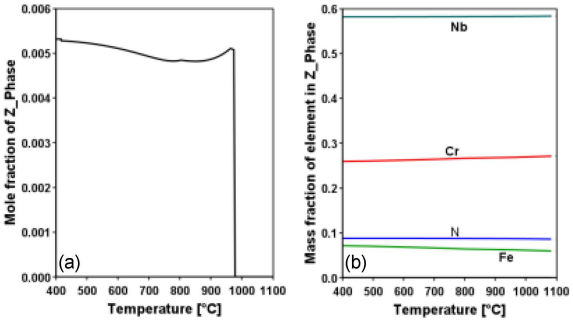


Fig. 5. Variation of (a) equilibrium mole fraction and (b) chemical composition of Z-phase in HR3C steel, as a function of temperature.

The changes in mole fraction and chemical composition of these phases as a function of temperature are shown in Figs. 3–5. One can see that they contain several crucial elements. The main constituent of $M_{23}C_6$ carbide is chromium, however, this carbide also contains iron and a small amount of nickel. The content of chromium in carbide increases as the temperature decreases. Iron, chromium and nickel are the main constituents of the $\sigma$-phase. The chemical composition of Z-phase includes niobium, chromium, iron and nitrogen.

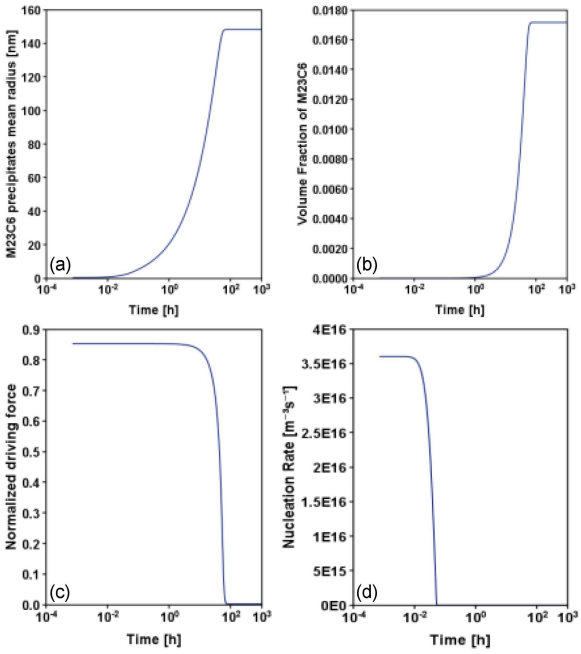


Fig. 6. Simulation of $M_{23}C_6$ carbide precipitation by TC-PRISMA: (a) particles mean radius, (b) particles volume fraction, (c) driving force for precipitation, (d) nucleation rate as a function of time.

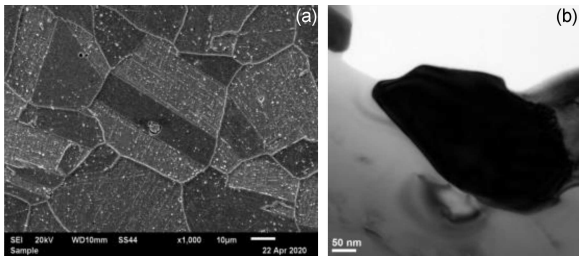


Fig. 7. (a) Microstructure and (b) the $M_{23}C_6$ carbide precipitation in HR3C steel after 100 h ageing at 700°C.

It must be emphasised that the ThermoCalc calculations are relevant for the state of equilibrium. For the materials used in the power generating industry, this state can be achieved in thousands of hours (this specifically refers to $\sigma$- and Z-phase) [7–9]. The precipitation process of $M_{23}C_6$ carbide, on the contrary, proceeds fast and will be followed in detail in this paper.

### 3.2. Kinetics simulation using TC-PRISMA

The microstructure investigation of the samples of HR3C steel has shown that profound precipitation of $M_{23}C_6$ carbide was detected during 100 and 500 h of ageing. Therefore, the simulation using TC-PRISMA was limited to this carbide. The precipitation process of $M_{23}C_6$ carbide was calculated at 700°C for 1000 h, and the simulation was performed with the assumption that the precipitates nucleate at grain boundaries. This is consistent with the microstructural observations. The most important parameter used in the simulation is interfacial energy. This parameter influences all the stages of the precipitation process. The value of this parameter varies from 0.016 to 0.265 J/m$^2$ [10]. The lowest values correspond to the coherent nucleation. In the calculation presented in this paper, the value of 0.23 J/m$^2$ was used for modelling the nucleation and growth process. The shape of the precipitates was assumed to be spherical. The results of $M_{23}C_6$ carbide precipitation process simulations with TC-PRISMA are shown in Fig. 6. It can be seen that the precipitation process starts as early as the ageing process starts. Figure 6 shows that after around 100 h, precipitation the process is ended.

### 3.3. Microstructure examinations

The HR3C steel in the as-received conditions was characterized by a typical austenitic microstructure with numerous annealing twins and numerous primary precipitates of different sizes arranged inside grains. The identification of precipitates revealed the existence of niobium-rich primary precipitations — NbX phase and Z-phase (NbCrN).

The changes in microstructure due to ageing at elevated temperature manifest themselves by secondary phase precipitation processes observed at the grain boundaries and inside the grains. $M_{23}C_6$ carbides were observed at the grain boundaries, while the dispersion precipitations of NbX and Z-phase were identified inside the grains (Fig. 7a). An example of the $M_{23}C_6$ carbide precipitation is shown in Fig. 7b. The particle diameter of $M_{23}C_6$ carbides after 100 h of ageing was 280 nm, and after 500 h it grew a little (to 300 nm). A detailed description of changes in the structure of HR3C steel is presented in the paper [11].

## 4. Discussion

The capability of the material behaviour modelling using the CALPHAD method was demonstrated in this paper, referring to the behaviour of HR3C austenitic steel during ageing at 700°C. Both the ThermoCalc and TC-PRISMA correctly predicted the equilibrium phases occurring in the steel and kinetics of $M_{23}C_6$ carbide precipitation. The simulation results obtained using TC-PRISMA showed that also the kinetics of the precipitation processes can accurately be predicted in complex systems. However, this type of modelling is more robust since the accuracy of prediction is dependent on many physical parameters that should be carefully adjusted. The interface energy is the most important parameter for the modelling. However, once the kinetics model is scaled, it can be used to extrapolate the long time performance of precipitates. This feature is specifically advantageous for the materials used in the power industry.

## 5. Conclusions

Microstructure investigation with STEM showed that the $M_{23}C_6$, NbX and Z-phases precipitations occurred during the ageing treatment of HR3C steel. The precipitation of $M_{23}C_6$ carbide nucleate at grain boundaries. The precipitations of NbX and Z-phase were observed inside the grains. The size of the precipitates $M_{23}C_6$ after 100 h did not differ substantially from the size of precipitates after 500 h of ageing and was around 300 nm. The simulation performed with TC-PRISMA showed that this is associated with a lowering in the driving force for precipitation, which finally resulted in growth suppression. The calculated chemical composition of the matrix and $M_{23}C_6$ carbides was comparable with the results of the calculations. Identification of the current precipitations carried out with the transmission electron microscope confirmed the results obtained using CALPHAD method.

## References


[1] G. Golański, A. Zieliński, M. Sroka, J. Słania, *Materials* **13**, 1297 (2020).

[2] T. Frolov, M. Asta, Y. Mishin, *Opin. Solid State Mater. Sci.* **20**, 308 (2016).

[3] H.L. Lukas, S.G. Fries, B. Sundman, *Computational Thermodynamics — The CALPHAD Method*, Cambridge University Press, 2007.

[4] J.J. Van Laar, *Z. Phys. Chem.* **63**, 216 (1908) (in German).

[5] J.J. Van Laar, *Z. Phys. Chem.* **64**, 257 (1908) (in German).

[6] L. Kaufman, *Acta Metall.* **15**, 575 (1959).

[7] G. Golański, *Żarowytrzymałe stale austenityczne*, Seria Monografie nr 73, Politechnika Częstochowska 2017 (in Polish).

[8] A. Zieliński, R. Wersta, M. Sroka, *Arch. Civ. Mech. Eng.* **22**, 1 (2022).

[9] G. Golański, A. Zieliński, M. Sroka, *Int. J. Press. Vessels Pip.* **188**, 104160 (2020).

[10] E. Trillo, L. Murr, *J. Mater. Sci.* **33**, 1263 (1998).

[11] A. Zieliński, G. Golański, M. Sroka, *Mater. Sci. Eng.* **796A**, 139944 (2020).